Desalination and Water Treatment
www.deswater.com
47 (2012) 78–85
September
1944-3994/1944-3986
doi: 10.1080/19443994.2012.696798
Taylor & Francis
Taylor & Francis Group

Phosphate adsorption on biogenetic calcium carbonate minerals: effect of a crystalline phase

Qiang Liu*, Lijing Guo, Yingmei Zhou, Yingchun Dai, Linlin Feng, Jizhi Zhou, Jun Zhao, Jianyong Liu, Guangren Qian*

School of Environmental and Chemical Engineering, Shanghai University, No. 99 Shangda Road, Shanghai 200444, P.R. China
Tel. +86 21 66137743, +86 21 66137758; Fax: +86 21 66137761; emails: qliu@shu.edu.cn; grqian@shu.edu.cn

Received 29 September 2011; Accepted 14 March 2012

ABSTRACT

The shells of *Argopecten irradians* (SAI) and *Mactra veneriformis* (SMW) were used as adsorbents to remove the phosphate from an aqueous solution in the present study. The removal kinetics and adsorption isotherms were investigated, and the phosphate adsorption behaviors by these two shells were also explored and discussed. The results indicated that the kinetic of an adsorption process follows the Lageren pseudo-first-order equation and the adsorption isotherm accords well with both the Langmuir and Freundlish adsorption equations, while the former is more suitable. Based on the Langmuir model, the monolayer saturated adsorption quantities of SAI and SWM at 25°C are 3.07 and 3.32 mmol/g, respectively. The phosphate adsorption on these shells is endothermic in nature and the adsorption capacities of such shells increase with temperature. In addition, biogenic calcium carbonate with a calcite phase shows more capacity on phosphate adsorption than the one with an aragonite phase.

Keywords: Calcite; Shells; Phosphate; Adsorption

1. Introduction

Phosphate is a major contaminant of concern in wastewater effluent, leading to eutrophication of water bodies. If the wastewater from industrial, agricultural, and domestic practice, with high concentrations of phosphate, is not adequately treated, then the release of phosphate to natural water could adversely affect the aquatic ecosystems.

In recent years, various methods including biological, physical, and chemical methods have been developed to remove phosphate from wastewater. Among such methods, adsorption is an effective and economic technique for phosphate removal. Several adsorbents including waste materials such as fly ash [1–4], red mud [5–7], alum sludge [8,9], and shells [10–14] as well as natural minerals such as goethite [15–17], hematite [18,19], palygorskites [20], dolomite [21–23], alunite [24], bentonite [25], calcite [26–33], and aragonite [34] have been investigated. These materials are easily accessible and can be obtained at a relatively low cost.

Calcite is an abundant polymorph of calcium carbonate. In natural water bodies, calcium carbonate can

*Corresponding authors.

act as a sink of phosphate. The existing literature suggests that the removal of phosphorus by calcium carbonate is a two-step process: phosphate chemisorption on calcite followed by a transformation of amorphous calcium phosphate to crystalline apatite [33]. The growth rate of an apatite crystal depends strongly on the phosphate/carbonate ratio due to competition in the crystal growth sites. The crystal structure of calcium carbonate can influence the adsorption behavior of phosphate to a large extent. It was found that the initial uptake rate of phosphate by aragonite (another common calcium carbonate mineral) is much larger than calcite [35]. The large difference in the phosphate adsorption rate may be due to the distinction of reaction sites (in the crystal lattice or in the specific surface area) [36]. For example, Burton and Walter [11] have found that $CaCO_3$ with different specific surface areas can cause the phosphate adsorption to vary by 3–7 folds.

Shells are made of a biogenic calcium carbonate mineral, which typically contains a much high percentage of $CaCO_3$ (95–99%, calcite or aragonite) by weight. A literature search indicates that oyster shells [10,11], crab shells [12] and scallop shells [14] were tested for the phosphate removal from an aqueous solution. Kwon et al. [10] found that the heated oyster shells possess a moderate phosphate removal ability, while the pulverized oyster shells achieve an excellent phosphate removal efficiency (up to 98%). However, the preparation of oyster shells (heating to 750˚C and pulverizing under 750˚C) requires a significant energy input. Jeon and Yeom [12] reported a much higher phosphate adsorption capacity (108.5 mg/g) of crab shells and found that the particle size has a great influence on the phosphate removal. While another biogenic calcium carbonate mineral, scallop shells just attained the maximum phosphate adsorption capacity of 23.0 mg/g, other parameters such as the shell size, temperature, and pH were found to have a major effect on phosphate removal [14]. Even though some beneficial results have been obtained on phosphate adsorption by biogenic calcium carbonate, few studies have focused on the effect of crystalline phase of calcium carbonate on the phosphate removal.

Argopecten irradians shells (calcite phase) and *Mactra veneriformis* shells (aragonite phase) are generated in large quantities by the manufacturers of marine products and these materials are usually thrown away as a restaurant waste in China. Based on the fact that these shells are mainly composed of calcium carbonate but are different in the crystalline phase, this experiment aims to investigate the adsorption behaviors of phosphate on biogenic calcite (*Argopecten irradians* shells) and biogenic aragonite (*Mactra veneriformis* shells) and analyze the adsorption mechanism of phosphate on these biogenic carbonates.

2. Materials and methods

2.1. Materials

The shells of *Argopecten irradians* (SAI) and shells of *Mactra veneriformis* (SMV) were used as adsorbents in this experiment to remove the phosphate from the aqueous solution. Calcite ($CaCO_3$ content > 99%) was obtained from Guangxi, China. The SAI and SMV were collected from Tongchuan Lu fisheries market, Shanghai, China. The collected shells were thoroughly washed three times with deionized water and dried in an oven at 70˚C. All samples were then finely crushed and sieved by a 150 mesh screen. The phosphate solutions were prepared by dissolving the AR grade KH_2PO_4 into deionized water. The pH of the phosphate solution was adjusted with 0.1 M HNO_3 and NaOH.

2.2. Adsorption studies

The batch adsorption experiments were carried out in 100 mL sealed conical flasks. Each conical flask was filled with 50 mL of phosphate solution. After a known amount of the adsorbent was added, the flasks were agitated in a temperature-controlled shaker (25˚C) at the rate of 100 rpm. At suitable intervals, aqueous samples were taken for phosphate and Ca^{2+} measurement. At the end of adsorption, the sorbents were withdrawn by filtration through a 0.45 μm membrane and dried for characterization.

2.3. Analysis methods

Aqueous pH was measured using a digital pH meter (Shanghai Precision Scientic Instrument Co., Ltd, Model pHS-3C, China). The phosphate and Ca^{2+} concentrations were determined by an inductively coupled plasma atomic emission spectrometer (ICP, Leeman, Model Prodigy, USA) following the EPA QA/QC standard methods. Infrared spectra of raw/used adsorbents were collected by the FTIR spectrum (Thermo Nicolet Corporation, Model AVATAR370, USA) in the range of 4,000–400 cm^{-1} with a resolution of 2 cm^{-1} using the KBr pellet technique.

3. Results and discussion

3.1. Adsorption kinetics

The adsorption kinetics experiments were performed with fixed initial phosphate concentrations

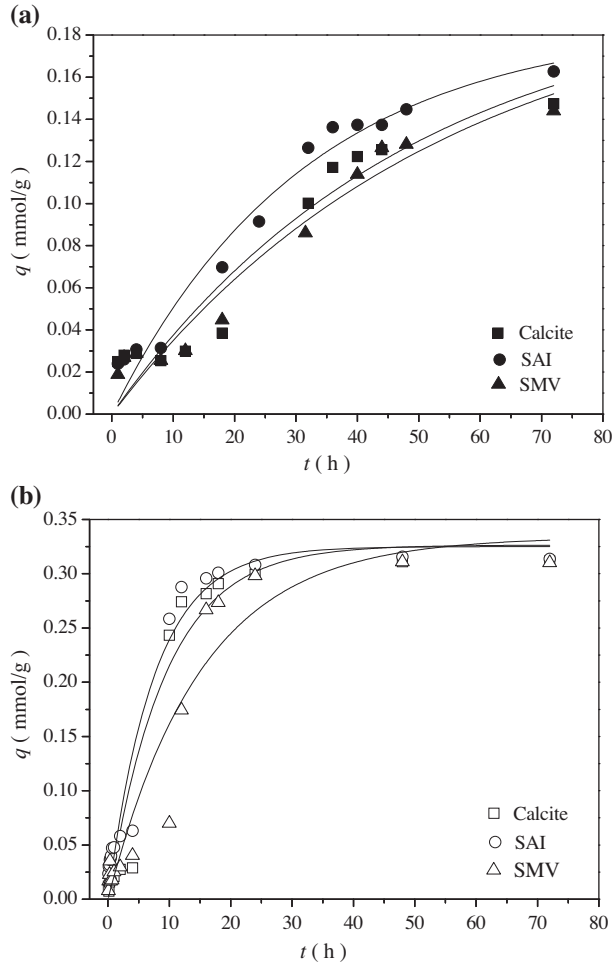

Fig. 1. The effect of contact time on the phosphate adsorption by calcite, SAI, and SMV (pH = 6.0, T = 25℃, adsorbent dosage = 0.10 g/50.0 mL). (a) $C_0 = 10.0$ mg/L, (b) $C_0 = 20.0$ mg/L.

($C_0 = 10.0$ and 20.0 mg/L) and an adsorbent dosage (0.10 g/50 mL) at the initial pH of 6.0 and temperature of 25℃.

The time-adsorption profiles of phosphate (Fig. 1) show that the adsorption process is clearly time dependent. Calcite, biogenic calcite (SAI), and biogenic aragonite (SMV) presented a similar trend of phosphate adsorption, while the removal efficiency of phosphate by biogenic calcite (SAI) was higher than those by calcite and biogenic aragonite (SMV).

As shown in Fig. 1(a), the adsorption of phosphate occurred rapidly at the initial stage and became slow after 40 h, while the equilibrium was not achieved within 72 h. At $C_0 = 20.0$ mg/L (Fig. 1(b)), phosphate adsorption capacities first increased sharply and then reached a saturated plateau within about 48 h. Based on this result, an adsorption cycle of 48 h was selected for $C_0 = 20.0$ mg/L.

The adsorption kinetics of phosphate data were analyzed using pseudo-first-order, pseudo-second-order, and Elovich models. These kinetic equations are shown as follows:

Pesudo-first-order equation

$$\ln(q_e - q_t) = \ln q_e - k_1 t \quad (1)$$

Pesudo-second-order equation

$$q_t = k_2 q_e^2 t/(1 + k_2 q_e t) \quad (2)$$

Elovich equation

$$q_t = A + B \ln t \quad (3)$$

where q_e (mmol/g) is the phosphate adsorbed at equilibrium, q_t (mmol/g) is the amount adsorbed at time t (h), k_1 (h^{-1}) and k_2 (g mol^{-1} h^{-1}) are the pseudo-first-order rate constant and pseudo-second-order rate constant, respectively, and A and B are the Elovich constants.

The results of fitting the experimental data to the three models are presented in Table 1. The phosphate adsorption in the present study most closely followed

Table 1
The parameters of an adsorption kinetic curve of the phosphate

Adsorbent	C_0 (mg L^{-1})	Pesudo-first-order kinetics			Pesudo-second-order kinetics			Elovich		
		q_e (mmol g^{-1})	k_1 (h^{-1})	R^2	q_e (mmol g^{-1})	k_2 (g $mmol^{-1}$ h^{-1})	R^2	A	B	R^2
Calcite	10.0	0.20	0.02	0.91	0.32	0.04	0.90	−0.007	0.03	0.69
	20.0	0.33	0.11	0.96	0.39	0.29	0.93	0.078	0.06	0.83
SAI	10.0	0.19	0.03	0.97	0.26	0.09	0.96	−0.006	0.04	0.85
	20.0	0.33	0.13	0.96	0.38	0.42	0.94	0.096	0.06	0.86
SMV	10.0	0.20	0.02	0.94	0.33	0.036	0.93	−0.009	0.03	0.74
	20.0	0.33	0.07	0.93	0.42	0.15	0.91	0.068	0.05	0.77

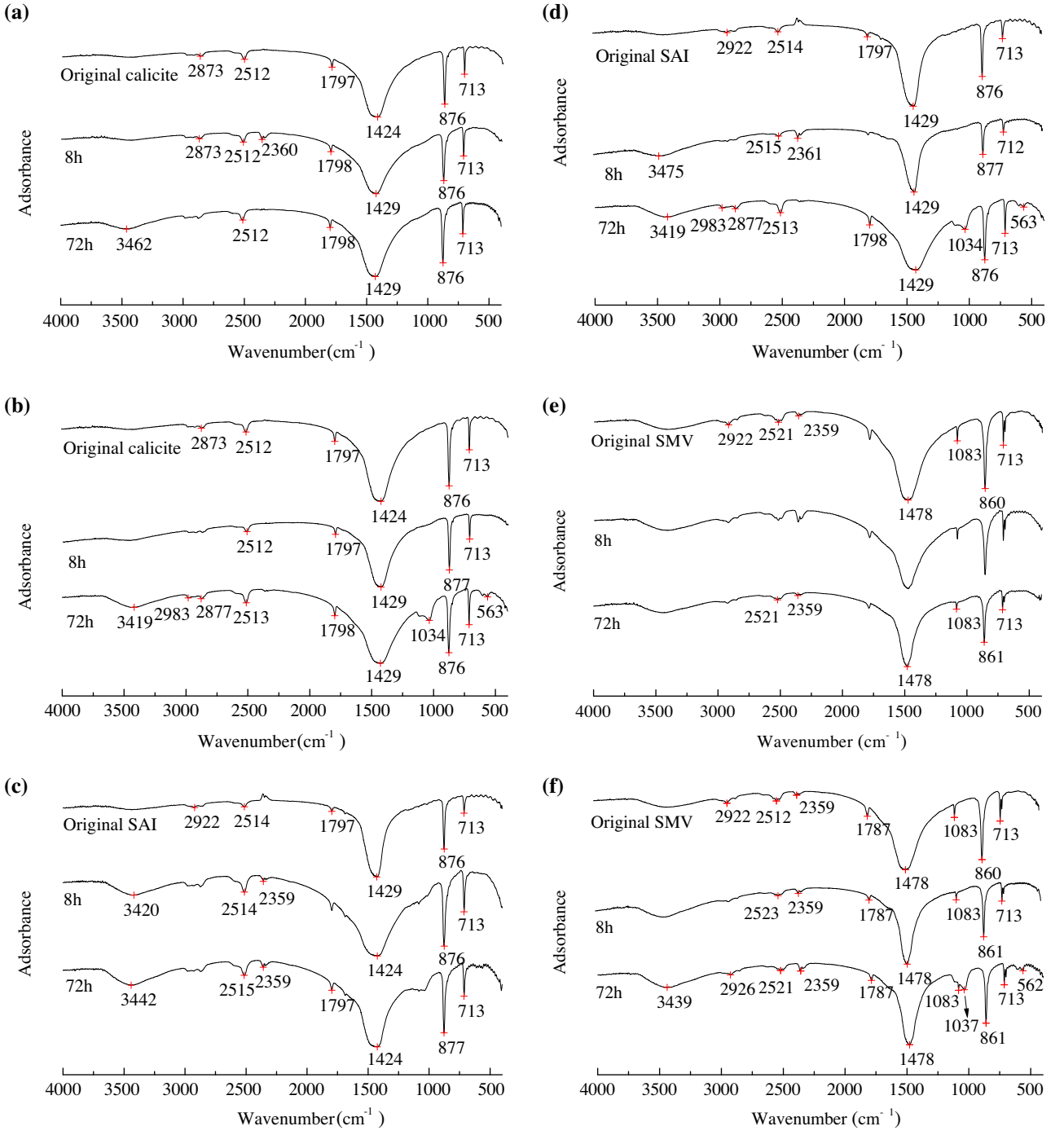

Fig. 2. The FTIR spectrum of adsorbents with different initial concentration and contact time; (a) calcite, C_0 = 10.0 mg/L; (b) calcite, C_0 = 20.0 mg/L; (c) SAI, C_0 = 10.0 mg/L; (d) SAI, C_0 = 20.0 mg/L; (e) SMV, C_0 = 10.0 mg/L; (f) SMV, C_0 = 20.0 mg/L.

pseudo-first-order kinetics, by which a very accurate estimation of q_e and the highest correlation coefficient ($R^2 > 0.91$) (Table 1) are achieved.

From Table 1, when C_0 = 10.0 mg/L, the values of k_1 for calcite, SAI, and SMV (0.02, 0.03, and 0.02 h^{-1}, respectively) showed little difference. However, when the initial phosphate concentration was elevated to 20.0 mg/L, values of k_1 for calcite, SAI, and SMV were 0.11, 0.13, and 0.07 h^{-1}, respectively, indicating that biogenic calcite is more advantageous,

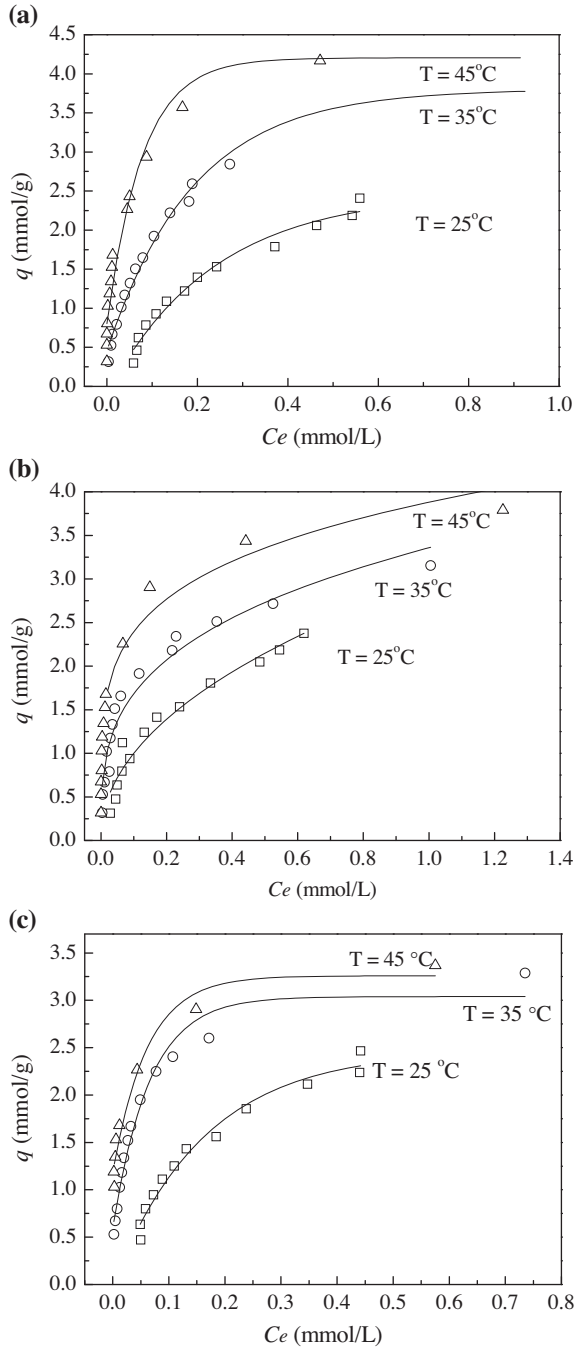

Fig. 3. Phosphate adsorption on (a) calcite, (b) SAI, and (c) SMV at different temperature (pH = 6.0, adsorbent dose = 0.10 g/50.0 mL, t = 48 h).

since k_1 stands for the reaction speed. With regard to the difference in the adsorption performance between the SAI and the SMV, it was tentatively inferred that calcite shows a higher solubility owing to which a higher concentration of Ca^{2+} occurs on the sorbent surface, leading to a better adsorption performance.

3.2. FTIR spectrum of raw/used adsorbent

In the adsorption kinetics experiments, infrared spectra of the raw and used adsorbents were collected and are shown in Fig. 2.

The FTIR spectrums of the raw calcite, SAI, and SMV indicated that these absorbents are mainly of high purity of calcium carbonate. According to Fig. 2 (a) and (c), calcite and SAI are calcite phase with characteristic vibrations at 713, 876, and 1,424 (or 1,429) cm^{-1}. While Fig. 2e shows that SMV is aragonite phase with the characteristic vibrations at 713, 860, and 1,478 cm^{-1} and ν_1 symmetric stretching vibrations (1,083 cm^{-1}) of calcium carbonate (aragonite) [11].

As shown in Fig. 2(a)–(e), after 8 or 72 h of adsorption (at C_0 = 10.0 mg/L), the O–H stretching vibration of $H_2PO_4^-$ at 2,359 cm^{-1} was observed on the FTIR spectrums of calcite, SAI, and SMV, indicating that dihydric phosphate was generated on these adsorbents' surface. The peak at 1,424 cm^{-1} is related to shifted v_3 ($CaCO_3$) asymmetrical stretching vibrations [11]. Hence, at C_0 = 10.0 mg/L, physical adsorption is the dominant mechanism in this experiment.

As regards Fig. 2(b)–(f), when the initial phosphate concentration was doubted to 20 g/L, no characteristic band, except for the O–H stretching vibration of $H_2PO_4^-$ and the shifted bands of $CaCO_3$, was detected at an adsorption time of 8 h. However, when the adsorption time was multiplied to 72 h, v_4 (PO_4^{3-}) deformation vibration and ν_3 (PO_4^{3-}) stretching vibration appeared. These vibrations characterized the existence of $CaHPO_4$ [11]. Therefore, it was inferred that chemical precipitation took place successively after phosphate physicsorption.

3.3. Adsorption isotherm

The adsorption equilibrium experiments were conducted at different initial phosphate concentrations which varied from 20.0 to 300.0 mg/L and the temperature of 25, 35, and 45℃ with an initial pH = 6.0. An adsorbent amount of 0.10 g (with 50.0 mL of phosphate solution) was selected and the adsorption cycle was fixed at 48 h.

Fig. 3 shows the effect of temperature on phosphate adsorption for different adsorbents. The adsorption capacities of phosphate on these materials increased with the increase of temperature, suggesting that this process is endothermic in nature. This result coincided with the phosphate adsorption on the iron hydroxide-eggshell waste [13], raw/activated red mud, and fly ash [35].

Table 2
Langmuir and Freundlich isotherm constants for phosphate adsorption

Adsorbent	Temperature (K)	Langmuir			Freundlich		
		Q (10^{-3} mol g^{-1})	B (g mol^{-1})	R^2	K_f (10^{-3} mol g^{-1})	n	R^2
Calcite	298	3.50	3229.2	0.99	3.55	1.55	0.98
	308	4.52	8433.8	1.00	4.66	2.27	0.99
	318	4.90	29732.6	1.00	4.52	4.31	0.98
SAI	298	3.07	4641.7	0.99	3.13	1.99	0.95
	308	3.58	12273.1	0.99	3.51	3.04	0.97
	318	4.64	19371.4	1.00	3.83	4.80	0.99
SMV	298	3.32	5333.6	0.99	3.88	1.83	0.98
	308	3.62	16317.6	1.00	3.93	3.49	0.96
	318	4.39	22057.1	1.00	3.64	5.84	0.99

The obtained experimental data were fitted to linearly transformed Langmuir equation and Freundich equation as shown in Eqs. (4) and (5) [36].

$$\frac{C_e}{x/m} = \frac{1}{bQ} + \frac{C_e}{Q} \tag{4}$$

where C_e is the equilibrium adsorption concentration in solution (mol/L), Q denotes the amount adsorbed per unit mass of adsorbent (mol/g) for monolayer coverage, x/m denotes the amount adsorbed per unit mass of adsorbent at equilibrium (mol/g), and b is a constant related to the affinity of the binding sites.

$$\log\frac{x}{m} = \log K_f + \frac{1}{n}\log C_e \tag{5}$$

where K_f gives the adsorption capacity of the adsorbent in mol/g, n shows the constant related to energy and intensity of adsorption.

The calculated Langmuir and Freundlich isotherm constants are presented in Table 2. Based on the correlation coefficient R^2, the Langmuir equation is much more suitable for the adsorption equilibrium data over the concentration range in this experiment. Therefore, it was tentatively inferred that the adsorption of phosphate on these adsorbents was of the monolayer type.

According to the calculated results based on the Langmuir equation, monolayer saturated adsorption quantities of the calcite at 25, 35, and 45°C were 3.50, 4.52, and 4.90 mmol/g, respectively. The SAI and the SMV showed slightly lower monolayer saturated adsorption quantities (3.07, 3.58, and 4.64 mmol/g for SAI and 3.32, 3.62, and 4.39 mmol/g for SMV at 25, 35, and 45°C, respectively). It was obvious that high temperature is favorable for the adsorption of phosphate on the carbonate. Meanwhile, according to the Freundlich equation, the constants b (representing the adsorption appetency) and n (representing the adsorption strength) increased significantly with the temperature, suggesting that the adsorption interaction is stronger at higher temperature.

The temperature-dependent adsorption process is associated with changes in several thermodynamic parameters, such as the changes of standard free energy (ΔG°), enthalpy (ΔH°), and entropy (ΔS°) of adsorption. According to Das et al. [36], the changes of standard free energy (ΔG°) can be calculated by following equation.

$$\Delta G^\circ = -RT\ln(b) \tag{6}$$

where R is the universal gas constant, T is the temperature (K), and b is the Langmuir constant. According to Van't Hoff model (Eq. (7)),

$$\ln(b) = \frac{\Delta S^\circ}{R} - \frac{\Delta H^\circ}{RT} \tag{7}$$

The values of ΔH° and ΔS° were evaluated from the slope and intercept of the Van't Hoff plot by the regression method and are shown in Table 3. The positive values of ΔH° confirm the endothermic nature of the adsorption process. The negative values of ΔG° at 298, 308, and 318 K indicate the spontaneous nature of phosphate adsorption. The positive values of ΔS° suggest the adsorption of phosphate on the calcite, SAI, and SMV lead to an increase in the randomness at the solid/solution interface.

3.3. Effect of the adsorbent dosage

Adsorbent dosage is another factor that influences the adsorption equilibrium. In the present

Table 3
Gibbs free energy, enthalpy, and entropy changes associated with the phosphate adsorption by the calcite, SAI, and SMV

Adsorbent	Temperature (K)	ΔG° (kJ mol^{-1})	ΔH° (kJ mol^{-1})	ΔS° (kJ mol^{-1} K^{-1})
Calcite	298	−20.01		
	308	−23.14	87.25	0.36
	318	−27.22		
SAI	298	−20.90		
	308	−24.10	56.46	0.26
	318	−26.08		
SMV	298	−21.25		
	308	−24.83	56.24	0.26
	318	−26.43		

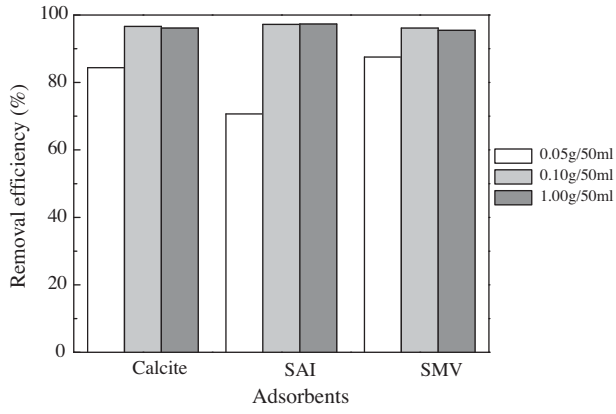

Fig. 4. The effect of adsorbent dose on the phosphate removal (pH = 6.0, T = 25℃, C_0 = 20.0 mg/L, t = 48 h).

study, the effect of adsorbent doses was investigated by conducting batch adsorption tests with different adsorbent amounts (0.05, 0.10, and 1.00 g per 50 mL of solution) with a phosphate concentration of 20.0 mg/L and an initial pH = 6.0. The adsorption temperature was fixed at 25℃ and the adsorption time as 48 h.

The effect of sorbent dosage on phosphate removal is shown in Fig. 4. As it can be seen, increasing the adsorbent dosage from 0.05 to 0.10 g led to a noticeable promotion of the phosphate removal, i.e. the removal efficiency of phosphate by the SAI increased from 75.2 to 97.8% when adsorbent dosage was doubled. This phenomenon can be easily explained with the increase of surface area, i.e. more active adsorption sites when more adsorbent is used. However, further elevating the adsorbent amount to 1 g, no apparent improvement in phosphate removal was detected. Thus, the adsorbent dosage of 0.10 g per 50 mL seems to be suitable.

4. Conclusion

The experimental results indicate that the SAI and SWM are both effective in phosphate removal. The kinetics of phosphate adsorption on the SAI and the SWM follows the pesudo-first-order kinetic and SAI shows a higher adsorption rate. The adsorption process agrees with both the Langmuir and Freundlich isotherms but the former is more appropriate. The monolayer saturated adsorption quantities of SAI and SWM are 3.07 and 3.32 mmol/g at 25℃, slightly inferior to calcite. Furthermore, the adsorption process is endothermic in nature and the adsorption capacities of two adsorbents increase with temperature.

Acknowledgments

This work was financially supported by the Science and Technology Council of Shanghai (Grant No. 092312802) and the Shanghai Leading Academic Disciplines (S30109).

Symbols

q_e	—	phosphate adsorbed at equilibrium, mmol/g
q_t	—	phosphate adsorbed at time t, h
k_1	—	pseudo-first-order rate constant, h^{-1}
k_2	—	pseudo-second-order rate constant, g mol^{-1} h^{-1}
A, B	—	the constant in Elovich kinetics equation
t	—	adsorption time, h
C_0	—	initial aqueous phosphate concentration, mg/L
C_e	—	aqueous phosphate concentration at equilibrium adsorption, mol/L
Q	—	the amount adsorbed per unit mass of the adsorbent for monolayer coverage, mol/g
x/m	—	the amount adsorbed per unit mass of the adsorbent at equilibrium, mol/g

b — constant in the Langmuir equation
K_f — adsorption capacity of the adsorbent, mol/g
n — the constant in the Freundich equation
ΔG° — changes in standard free energy before and after adsorption, kJ/mol
ΔH° — the changes in standard entropy before and after adsorption, kJ/mol
ΔS° — the changes in standard entropy before and after adsorption, $kJ\,mol^{-1}\,K^{-1}$
R — the universal gas constant, $J\,mol^{-1}\,K^{-1}$
T — Temperature, K

References

[1] E. Oguz, Sorption of phosphate from solid/liquid interface by fly ash, Colloids Surf., A PEAEH. 262 (2005) 113–117.
[2] J. Chen, H. Kong, D. Wu, X. Chen, D. Zhang, Z. Sun, Phosphate immobilization from aqueous solution by fly ashes in relation to their composition, J. Hazard. Mater. 139 (2007) 293–300.
[3] S.G. Lu, S.Q. Bai, L. Zhu, H.D. Shan, Removal mechanism of phosphate from aqueous solution by fly ash, J. Hazard. Mater. 161 (2009) 95–101.
[4] S.S. Choi, J.H. Chung, S.H. Yeom, Removal of phosphate using coal fly ash from a thermal power station, J. Ind. Eng. Chem. 11 (2005) 638–642.
[5] E. López, B. Soto, M. Arias, A. Núñez1, D. Rubinos, M.T. Barral, Adsorbent properties of red mud and its use for wastewater treatment, Water Res. 32 (1998) 1314–1322.
[6] J. Pradhan, J. Das, S. Das, R.S. Thakur, Adsorption of phosphate from aqueous solution using activated red mud, J. Colloid Interface Sci. 204 (1998) 169–172.
[7] W. Huang, S. Wang, Z. Zhua, L. Li, X. Yao, V. Rudolph, F. Haghseresht, Phosphate removal from wastewater using red mud, J. Hazard. Mater. 158 (2008) 35–42.
[8] S.H. Huang, B. Chiswell, Phosphate removal from wastewater using spent alum sludge, Water Sci. Technol. 42 (2000) 295–300.
[9] Y. Yang, Y.Q. Zhao, A.O. Babatunde, L. Wang, Y.X. Ren, Y. Han, Characteristics and mechanisms of phosphate adsorption on dewatered alum sludge, Sep. Purif. Technol. 51 (2006) 193–200.
[10] H.B. Kwon, C.W. Lee, B.S. Jun, J. Yun, S.Y. Weon, B. Koopman, Recycling waste oyster shells for eutrophication control, Resour. Conserv. Recy. 41 (2004) 75–82.
[11] C. Namasivayam, A. Sakoda, M. Suzuki, Removal of phosphate by adsorption onto oyster shell powder—kinetic studies, J. Chem. Technol. Biotechnol. 80 (2005) 356–358.
[12] D.J. Jeon, S.H. Yeom, Recycling wasted biomaterial, crab shells, as an adsorbent for the removal of high concentration of phosphate, Bioresour. Technol. 100 (2009) 2646–2649.
[13] N.Y. Mezenner, A. Bensmaili, Kinetics and thermodynamic study of phosphate adsorption on iron hydroxide-eggshell waste, Chem. Eng. J. 147 (2009) 87–96.
[14] S.H. Yeom, K.Y. Jung, Recycling wasted scallop shell as an adsorbent for the removal of phosphate, J. Ind. Eng. Chem. 15 (2009) 40–44.
[15] R. Chitrakar, S. Tezuka, A. Sonoda, K. Sakane, K. Ooi, T. Hirotsu, Phosphate adsorption on synthetic goethite and akaganeite, J. Colloid Interface Sci. 298 (2006) 602–608.
[16] C. Luengo, M. Brigante, J. Antelo, M. Avena, Kinetics of phosphate adsorption on goethite: Comparing batch adsorption and ATR-IR measurements, J. Colloid Interface Sci. 300 (2006) 511–518.
[17] B. Zhong, R. Stanforth, S. Wu, J.P. Chen, Proton interaction in phosphate adsorption onto goethite, J. Colloid Interface Sci. 308 (2007) 40–48.
[18] X. Huang, Intersection of isotherms for phosphate adsorption on hematite, J. Colloid Interface Sci. 271 (2004) 296–307.
[19] E.J. Elzinga, D.L. Sparks, Phosphate adsorption onto hematite: An *in situ* ATR-FTIR investigation of the effects of pH and loading level on the mode of phosphate surface complexation, J. Colloid Interface Sci. 308 (2007) 53–70.
[20] H. Ye, F. Chen, Y. Sheng, G. Sheng, J. Fu, Adsorption of phosphate from aqueous solution onto modified palygorskites, Sep. Purif. Technol. 50 (2006) 283–290.
[21] H. Roques, L. Nugroho-Jeudy, A. Lebugle, Phosphorus removal from wastewater by half-burned dolomite, Water Res. 25 (1991) 959–965.
[22] S. Karaca, A. Gürses, M. Ejder, M. Açıkyıldız, Kinetic modeling of liquid-phase adsorption of phosphate on dolomite, J. Colloid Interface Sci. 277 (2004) 257–263.
[23] S. Karaca, A. Gürses, M. Ejdera, M. Açıkyıldız, Adsorptive removal of phosphate from aqueous solutions using raw and calcinated dolomite, J. Hazard. Mater. 128 (2006) 273–279.
[24] M. Özacar, Adsorption of phosphate from aqueous solution onto alunite, Chemosphere 51 (2003) 321–327.
[25] A. Dimirkou, A. Ioannou, M. Doula, Preparation, characterization and sorption properties for phosphates of hematite, bentonite and bentonite-hematite systems, Adv. Colloid Interface Sci. 97 (2002) 37–60.
[26] W.A. House, H. Casey, L. Donaldson, S. Smith, Factors affecting the coprecipitation of inorganic phosphate with calcite in hardwaters—I Laboratory studies, Water Res. 20 (1986) 917–922.
[27] J. Kleiner, Coprecipitation of phosphate with calcite in lake water: A laboratory experiment modelling phosphorus removal with calcite in Lake Constance, Water Res. 22 (1988) 1259–1265.
[28] W.A. House, The prediction of phosphate coprecipitation with calcite in freshwaters, Water Res. 24 (1990) 1017–1023.
[29] A.M. Hartley, W.A. House, M.E. Callow, B.S.C. Leadbeater, Coprecipitation of phosphate with calcite in the presence of photosynthesizing green algae, Water Res. 31 (1997) 2261–2268.
[30] L.J. Plant, W.A. House, Precipitation of calcite in the presence of inorganic phosphate, Colloids Surf., A PEAEH 203 (2002) 143–153.
[31] A.T. Kan, G. Fu, M.B. Tomson, Adsorption and precipitation of an aminoalkylphosphonate onto calcite, J. Colloid Interface Sci. 281 (2005) 275–284.
[32] K. Karageorgiou, M. Paschalis, G.N. Anastassakis, Removal of phosphate species from solution by adsorption onto calcite used as natural adsorbent, J. Hazard. Mater. 139 (2007) 447–452.
[33] L. Lv, J. He, M. Wei, X. Duan, Kinetic studies on fluoride removal by calcined layered double hydroxides, Ind. Eng. Chem. Res. 45 (2006) 8623–8628.
[34] Y. Li, C. Liu, Z. Luan, X. Peng, C. Zhu, Z. Chen, Z. Zhang, J. Fan, Z. Jia, Phosphate removal from aqueous solutions using raw and activated red mud and fly ash, J. Hazard. Mater. 137 (2006) 374–383.
[35] F. Millero, F. Huang, X.R. Zhu, X.W. Liu, J.Z. Zhang, Adsorption and desorption of phosphate on calcite and aragonite in seawater, Aquat. Geochem. 7 (2001) 33–56.
[36] J. Das, B.S. Patra, N. Baliarsingh, K.M. Parida, Adsorption of phosphate by layered double hydroxides in aqueous solutions, Appl. Clay Sci. 32 (2006) 252–260.